

Local Density of States for Individual Energy Levels in Finite Quantum Wires

Imke Schneider, Alexander Struck, Michael Bortz, and Sebastian Eggert

*Department of Physics and Research Center OPTIMAS,
Univ. Kaiserslautern, D-67663 Kaiserslautern, Germany*

(Dated: March 11, 2019)

The local density of states (LDOS) in finite quantum wires is calculated as a function of discrete energies and position along the wire. By using a combination of numerical density matrix renormalization group (DMRG) calculations and analytical bosonization techniques it is possible to obtain a complete understanding of the local spectral weights along the wire in terms of the underlying many particle excitations.

PACS numbers: 71.10.Pm, 73.21.Hb, 73.63.-b

There has been increasing interest in quasi one-dimensional quantum wires over the last few decades. Tunneling experiments have revealed signatures of strong correlations in different setups ranging from a powerlaw behavior of the temperature dependent conductance in carbon nanotubes [1, 2] to being able to map out the momentum resolved tunneling in parallel quantum wires in a GaAs/AlGaAs heterostructure [3, 4, 5]. By now the local tunneling density near nanotube edges can be measured fully resolved in energy and position [6], which has been interpreted as the interference pattern of collective excitations. Standing waves at discrete energies corresponding to the few lowest lying levels have also been observed in finite tubes with screened interactions [7, 8]. It can be expected that similar experiments will be able to identify collective excitations in short finite wires if the screening from the substrate can be reduced.

From the theoretical side the central quantity of interest is the local density of states (LDOS) of inserting one particle at position x to reach an excited state $|\omega_n\rangle$ with $N_0 + 1$ particles from the ground state $|N_0\rangle$

$$\begin{aligned}\rho(\omega, x) &= \sum_n |\langle \omega_n | \psi_x^\dagger | N_0 \rangle|^2 \delta(\omega - \omega_n) \\ &= -\frac{1}{\pi} \text{Im} \int_0^\infty e^{i\omega t} G^R(t, x) dt.\end{aligned}\quad (1)$$

Using the Luttinger liquid formalism it is now well understood how the scaling laws of the LDOS and the correlation functions are affected by boundaries [9, 10, 11, 12, 13, 14, 15]. The position resolved LDOS in finite wires was considered in Ref. [16] for the lowest few levels assuming a perfect degeneracy in the Luttinger liquid model.

From the numerical side it is surprising that so far only very few works [17] were able to analyze the DOS in interacting lattice models exactly. Part of the difficulty appears to be that the LDOS in Eq. (1) is related to the time-dependent retarded Green's function $G^R(t)$. In dynamical DMRG methods dramatic progress has been made over the past few years. Recently, it was possible to determine the spectral function as a function of the photoemission wavevector [17]. Unfortunately, indi-

vidual levels have not yet been resolved due to a finite correlation time or a finite cutoff in the Lehmann representation of the Green's function. To our knowledge there have been no numerical calculations for the LDOS in interacting lattice models so far.

In this paper, we are now able to quantitatively calculate the LDOS of a finite quantum wire by using a combination of bosonization and DMRG techniques [18]. In the numerical DMRG calculations we follow a direct approach, by targeting several excited states $|\omega_n\rangle$ in the sector with one additional fermion on top of the ground state. Keeping track of the particle number and all the anticommuting transition operators ψ_x^\dagger it is then possible to evaluate the matrix elements of the LDOS in Eq. (1) with very good spatial and energy resolution compared to calculating the DOS via the Green's function. Using bosonization a general analytic formula for the LDOS of nearly degenerate states is derived. The combination of numerical and analytical calculations gives a complete understanding of the distribution of spectral weights over individual states. The well-known powerlaws, however, can only be observed after a summation over nearly degenerate levels. The effect of spin is also discussed.

We consider interacting spinless fermions hopping on a finite wire with L sites and "open" ($\psi_0 = \psi_{L+1} = 0$) boundary conditions

$$H = -t \sum_{x=1}^{L-1} (\psi_x^\dagger \psi_{x+1} + h.c.) + U \sum_{x=1}^{L-1} n_x n_{x+1}, \quad (2)$$

where $n_x =: \psi_x^\dagger \psi_x$. This is the simplest model that illustrates Luttinger liquid physics for $-2t < U \leq 2t$ and is often used to describe quantum wires. It is believed that the results can be generalized to systems with spin as will be discussed later. Tunneling one single particle (or hole) into the wire will create excited states that may in general involve several more fermions (i.e. a so-called "single particle" excitation may still be a many body entangled state). In order to illustrate the nature of such many body excitations, consider the system without interaction ($U = 0$) first. In that case, eigenstates are created from the vacuum by creation operators

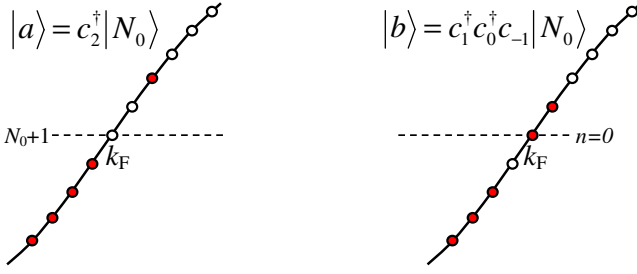


FIG. 1: (color online) Single particle excitations on the filled Fermi sea for the non-interacting system.

$c_n^\dagger = \sqrt{\frac{2}{L+1}} \sum_x \psi_x^\dagger \sin(k_n + k_F)x$, where the wavevector $k_n = n\frac{\pi}{L+1}$ is measured relative to the Fermi point k_F . For convenience $k_F = (N_0 + 1)\frac{\pi}{L+1}$ is chosen so that the number of particles in the filled Fermi sea is given by N_0 and there is no charging energy to the $N_0 + 1$ particle sector as indicated in Fig. 1. A typical example of a single-particle excitation in a tunneling experiment is the creation of one fermion above the filled Fermi sea $|a\rangle = c_2^\dagger |N_0\rangle$ as shown in Fig. 1. In that case, the LDOS in Eq. (1) is simply given by the square of the corresponding standing wave. A second example of a possible excitation $|b\rangle = c_1^\dagger c_0^\dagger c_{-1} |N_0\rangle$ is shown in Fig. 1, where also one additional fermion is created and another one has been excited from the Fermi sea. For non-interacting fermions the overlap matrix elements $\langle b | \psi_x^\dagger | N_0 \rangle$ of this many body excited state vanish in the LDOS Eq. (1), but this is no longer true for the interacting case. Note, that if the dispersion relation was exactly linear, the states $|a\rangle$ and $|b\rangle$ would be degenerate. However, in any realistic finite lattice model band curvature and interaction effects will cause a small energy splitting of higher order in $1/L$.

In order to treat local interactions with the Luttinger liquid formalism, we use an explicit description in terms of shifting operators [19], which is more convenient for finite size systems than a field theory approach. Shifting operators ϱ_n for $n \neq 0$ are defined $\varrho_n = \sum_\ell c_{\ell+n}^\dagger c_\ell$, which obey bosonic commutation relations $[\varrho_{-n}, \varrho_{n'}] = n\delta_{n,n'}$ on the infinitely continued spectrum assuming that all physically relevant states exist below a given cutoff. The zero mode $\varrho_0 = \sum_\ell (c_\ell^\dagger c_\ell - \langle c_\ell^\dagger c_\ell \rangle_{k_F})$ counts the number of particles relative to the filled Fermi sea. It is possible to create any state in a sector with a given particle number in terms of the ϱ_n . For example, we find by combinatorial methods that the addition of one fermion is represented by the following superposition of many body bosonic states

$$c_n^\dagger |N_0\rangle = \sum_{\sum_\ell \ell m_\ell = n} \prod_\ell \frac{1}{m_\ell!} \left(\frac{\varrho_\ell}{\ell}\right)^{m_\ell} |0\rangle, \quad (3)$$

where $|0\rangle$ represents the ground state with $N_0 + 1$

fermions. Here, the sum runs over occupation numbers m_ℓ which correspond to all possible partitions [20] of $n = \sum_\ell \ell m_\ell$ (e.g. for $n = 3 = 2 + 1 = 1 + 1 + 1$ there are three possible partitions). In particular, the states in Fig. 1 are given by

$$|a/b\rangle = \frac{1}{2} (\varrho_1^2 \pm \varrho_2) |0\rangle. \quad (4)$$

The local addition of one fermion is described by $\psi_x^\dagger \approx e^{-ik_F x} \varrho_L^\dagger(x) - e^{ik_F x} \varrho_R^\dagger(-x)$, where

$$\varrho_R^\dagger(x) = c(x) \exp\left(\sum_{n>0} e^{-ik_n x} \frac{\varrho_n}{n}\right) \exp\left(\sum_{n<0} e^{-ik_n x} \frac{\varrho_n}{n}\right) \quad (5)$$

in accordance with open boundary conditions [9, 10, 11, 12]. Here, the prefactor $c(x) = \frac{i}{\sqrt{2(L+1)}} e^{i(\phi_0 - \varrho_0 \frac{\pi x}{L+1})}$ also contains the zero mode operators ϱ_0 and ϕ_0 , which exactly create the $(N_0 + 1)$ -particle ground state $|0\rangle = e^{i(\phi_0 - \varrho_0 \frac{\pi x}{L+1})} |N_0\rangle$. The ambitious reader may enjoy verifying that the state in Eq. (3) is normalized and that the free fermion result $|\langle N_0 | c_n \psi_x^\dagger | N_0 \rangle|^2 = \frac{2}{L+1} |\sin(k_F + k_n)x|^2$ can also be evaluated in the boson language using Eq. (3) and (5).

It is normally assumed that the fermionic spectrum is linear for small energies, because in that case the many body excitations are exactly quantized with energy levels $\omega_n = v_F k_n$. Accordingly, the spectrum becomes remarkably simple $E - E_0 = \frac{\pi v_F}{L+1} \sum_{\ell=1}^{\infty} \ell m_\ell$, where $m_\ell = \langle \varrho_\ell \varrho_{-\ell} \rangle / \ell$ is an integer representing a boson occupation number and E_0 is the energy of the $(N_0 + 1)$ -particle ground state $|0\rangle$. The degeneracy of each level ω_n is given by the number of possible partitions of $n = \sum_\ell \ell m_\ell$. However, in this work we keep track of the exact spectrum of the finite lattice model, which is never exactly linear. The degeneracy is therefore lifted with an interesting distribution of spectral weights as we will see in the DMRG results.

In the bosonized language, interactions are described by a Bogoliubov transformation $\varrho_n = \alpha \tilde{\varrho}_n + \beta \tilde{\varrho}_{-n}$ where the rescaling parameters $\alpha = \frac{1}{2}(1/\sqrt{K} + \sqrt{K})$ and $\beta = \frac{1}{2}(1/\sqrt{K} - \sqrt{K})$ are characterized by the Luttinger liquid parameter K . For the model in Eq. (2), K and the Fermi velocity v_F are known exactly as a function of U by comparison with Bethe ansatz, e.g. at half filling $1/2K = 1 - \arccos(U/2t)/\pi$ and $v_F = 2tK \sin(\pi/2K)/(2K - 1)$. Up to higher order corrections, the model becomes diagonal in the newly defined operators $\tilde{\varrho}_n$, but the boson vacuum and all eigenstates correspond to complicated many-fermion superpositions. The ϱ_n in the local creation operator in Eq. (5) are rotated accordingly. After normal ordering the prefactor becomes

$$c(x) = \frac{i}{\sqrt{2(L+1)}} \left(\frac{\pi}{L+1} a\right)^{\beta^2} \left(2 \sin \frac{\pi}{L+1} x\right)^{\alpha\beta} \quad (6)$$

where the inconsequential zero modes are left out. Here a is a so-called cutoff parameter of order one lattice con-

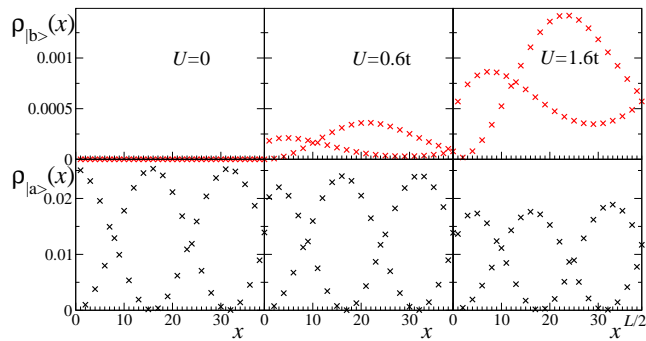


FIG. 2: (Color online) DMRG data for the LDOS $|\langle b|\psi^\dagger(x)|N_0\rangle|^2$ (first row) and $|\langle a|\psi^\dagger(x)|N_0\rangle|^2$ for $L = 78$, where $|b\rangle$ and $|a\rangle$ are eigenstates that have evolved from the $n = 2$ states in Fig. 1 when interactions U are switched on. The spectral weight is shifted towards $|b\rangle$ with increasing interactions, but $|a\rangle$ remains the dominant one.

stant, which comes from a sum over physical states and can be determined numerically as we will see below.

A "total" LDOS for a level ω_n can be defined as the sum over all nearly degenerate states $\rho_n(x) = \int_{\omega \approx \omega_n} \rho(\omega, x) d\omega$. We obtain the general analytic expression for $\rho_n(x)$ by summing over bosonic eigenstates $\prod_{\ell=1}^n (\ell^{m_\ell} m_\ell!)^{-1/2} \tilde{\varrho}_\ell^{m_\ell} |0\rangle$, corresponding to all partitions of $n = \sum_\ell \ell m_\ell$

$$\rho_n(x) = |c(x)|^2 \sum_{n=\sum \ell m_\ell} \left| \prod_{\ell=1}^n \frac{\chi_\ell^{m_\ell}}{\sqrt{\ell^{m_\ell} m_\ell!}} e^{ik_F x} - c.c. \right|^2 \quad (7)$$

where $\chi_\ell(x) = \alpha e^{ik_\ell x} + \beta e^{-ik_\ell x}$. This formula is the analytic generalization of the LDOS that was found for the first three levels in Ref. [16]. The LDOS shows a pattern of standing oscillations that are modified by collective bosonic excitations in the form of characteristic density waves as shown e.g. in Fig. 3. However, it must be remembered that the sum in Eq. (7) runs over several distinct many body states which are not exactly degenerate. Moreover, the linear combinations of the exact eigenstates is not known from bosonization. Therefore, numerical methods must be used to calculate the accurate behavior of the LDOS of the individual levels.

In the DMRG calculations we implement the model in Eq. (2) with $L = 78$ sites and $N_0 + 1 = 40$. As interactions are switched on, the ground state and excited states like $|a\rangle$ and $|b\rangle$ in Fig. 1 become complicated many-fermion states, but remain relatively simple in terms of the bosons. Figure 2 shows how the LDOS of the nearly degenerate eigenstates $|a\rangle$ and $|b\rangle$ changes with U . In particular, the spectral weight of the many-body state $|b\rangle$ increases with interactions. From the shape of the LDOS we can calculate the eigenstates in terms of bosonic excitations, e.g. $|a\rangle \approx (0.46\tilde{\varrho}_1^2 + 0.54\tilde{\varrho}_2)|0\rangle$ for $U = 1.6t$.

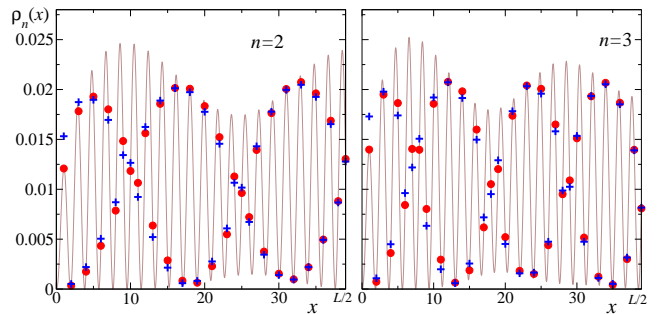


FIG. 3: (Color online) DMRG data for the total LDOS of level $n = 2$ for $U = 1.4t$ (blue crosses) compared to the bosonization results in Eq. (7) with $a = 0.56$ (solid line). Red dots mark the LDOS from bosonization at discrete lattice points.

The corresponding DMRG eigenenergies E_a and E_b agree very well with Bethe Ansatz calculations. For small interactions we have $E_a < E_b$ as expected from the curvature in the dispersion depicted in Fig. 1, while $E_a > E_b$ for larger interactions ($U \gtrsim 0.67t$ for $L = 78$) due to higher order operators.

The *total* LDOS ρ_n of nearly degenerate levels at a given ω_n can be compared with the analytical result in Eq. (7) as shown in Fig. 3 for $n = 2$ and for $n = 3$ in a wire with $U = 1.4t$. The overall scale is the only adjustable parameter, which determines the cutoff in Eq. (6), which ranges from $a = 0.3 \dots 0.6$ as $U = 0.2 \dots 1.6t$ is increased. Note, that the lattice structure of the model (2) is incommensurate with the rapid oscillations of the LDOS, which leads to a beating of the signal. The quantitative agreement with the analytical prediction is very good up to small deviations near the boundary.

It is in principle possible to perform the corresponding analysis for higher eigenstates by identifying the nearly degenerate "multiplets" for each discrete energy ω_n . However, the number of states in each multiplet n increases rapidly $\sim \exp(\pi\sqrt{2n/3})/4n\sqrt{3}$. We use a multitarget DMRG, including a variant of the Davidson algorithm [21], which is capable of calculating eigenstates of arbitrary given energy. Using the Bethe ansatz for determining the required energies, we were able to resolve the LDOS of the lowest 12 levels, which illustrates the behavior very well. The corresponding integrated spectral weights $\rho(\omega) = \sum_x \rho(\omega, x)$ for each level are shown in Fig. 4 for $U = 1.4t$. The spectral weights are distributed over all levels in each multiplet, so that a powerlaw as a function of energy is not obviously visible. We always find one dominant spectral weight in each multiplet which has evolved from the original single particle excitation in Eq. (3) ("type $|a\rangle$ "). The *total* spectral weight ρ_n of each multiplet agrees very well with the analytical results in Eq. (7). For ρ_n it is again possible to recognize approxi-

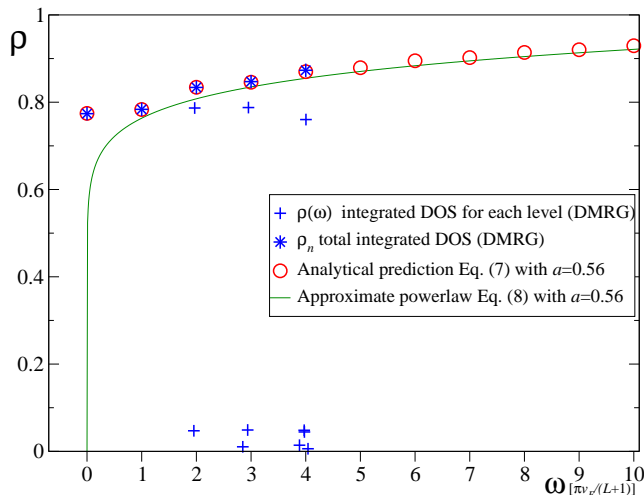


FIG. 4: (Color online) Numerical data for the integrated DOS $\rho(\omega) = \sum_x \rho(\omega, x)$ for each level at $U = 1.4t$ and $L = 78$. The dominant spectral weight at each multiplet corresponds to the single particle excitation of type $|a\rangle$. The total spectral weight ρ_n for each multiplet agrees very well with the Luttinger liquid prediction by summing over all sites in Eq. (7).

mate powerlaws

$$\rho_n \approx \frac{1}{\Gamma(1+2\beta^2)} \left(\frac{\pi a}{L+1} n \right)^{2\beta^2} = \frac{1}{\Gamma(1+2\beta^2)} \left(\frac{a}{v_F} \omega_n \right)^{2\beta^2}. \quad (8)$$

The remnants of additional oscillations with $\sin 2\omega x/v_F$ [14] in the semi-infinite case are now visible as a small alternation with n in Fig. 4. The low energy theory breaks down when the cutoff is approached $\omega \sim v_F/a$, i.e. before the DOS reaches the non-interacting value of unity. Interestingly, for the model in Eq. (2) the description in terms of a single cutoff a works remarkably well, describing both the range of validity and the normalization. In general, for longer range interactions it is also possible to use a momentum dependent Luttinger liquid parameter [22].

The situation as shown in Fig. 4 is actually quite generic for interacting systems also in higher dimensions: The single particle spectral weight is spread over many-body excitations, thereby renormalizing position, width, and total weight. The advantage of the current model is that a quantitative analysis can be made, which illustrates the behavior in detail.

In one-dimensional systems with spin degrees of freedom $\sigma = \uparrow, \downarrow$, the excitations can be described by two independent bosonic theories for spin and charge [19]. The spectrum is again given in the form of nearly degenerate multiplets $\omega = \omega_{n_s} + \omega_{n_c}$, but now labeled by two quantum numbers (n_s, n_c) for spin and charge with $\omega_{n_s} = v_s k_{n_s}$ and $\omega_{n_c} = v_c k_{n_c}$, where $v_c = v_s$ in the non-interacting case. A single particle state $c_{n,\sigma}^\dagger |N_0\rangle$ is now divided over all spin and charge multiplets (n_s, n_c) corresponding to the different possibilities to write the sum

$n = n_s + n_c$. However, for a given $n = n_s + n_c$ the multiplets (n_s, n_c) may now be of quite different energy, since in general $v_c > v_s$ for repulsive interactions. The spectral weight is therefore spread into several *non-degenerate* spin and charge multiplets, which is fundamentally different from higher dimensional systems. Moreover, the degeneracy within each multiplet is also lifted in the same fashion as above. In each multiplet there is again exactly one dominant state, which however only contains a small fraction of the single particle state. The LDOS also shows a very interesting superposition of spin and charge density waves [16], which can be calculated in detail with rescaled waves $\chi_\ell(x)/\sqrt{2}$ in Eq. (7). However, the smoking gun for Luttinger liquid behavior in a finite wire would be to identify the increasing number of states due to spin-charge separation and the degeneracy splitting with increasing ω , which is very different from an equally spaced single particle spectrum.

In summary, we were able to describe the LDOS for finite quantum wires in detail by a combination of analytical and numerical methods. The analytical results allow the calculation of the total LDOS in each multiplet. The DMRG calculations give the detailed distribution of local spectral weights over all many particle states in the low energy region. The combination of both methods shows explicitly how the wavefunctions and boson representations of single particle and many particle states evolve as interactions are turned on. The cutoff parameter $a(U)$ and the normalization in Eq. (6) can be determined from DMRG for the standard model in Eq. (2). Our results show that powerlaws are not sufficient to adequately describe the low energy behavior in finite wires. Instead, a large number of discrete states with varying spectral weights and oscillating wavefunctions would be the generic signature of Luttinger liquid behavior in finite wires. The number of many-particle states with non-zero spectral weight is small for the first few levels, but increases exponentially with energy.

Acknowledgments We are grateful to M. Andres and S. Söfing for helpful discussions and the SFB/Transregio 49 for financial support. I. S. acknowledges support of the Graduate Class of Excellence MATCOR funded by the State of Rheinland-Pfalz, Germany.

-
- [1] M. Bockrath, D.H. Cobden, J. Lu, A.G. Rinzler, R.E. Smalley, L. Balents, and P.L. McEuen, *Nature* **397**, 598 (1999).
 - [2] Z. Yao, H.W. Ch. Postma, L. Balents, and C. Dekker, *Nature* **402**, 273 (1999).
 - [3] O.M. Auslaender, H. Steinberg, A. Yacoby, Y. Tserkovnyak, B.I. Halperin, K.W. Baldwin, L.N. Pfeiffer, and K.W. West, *Science* **308**, 88, (2005).
 - [4] O.M. Auslaender, A. Yacoby, R. de Picciotto, K.W. Bald-

- win, L.N. Pfeiffer, and K.W. West, *Science* **295**, 825, (2002).
- [5] H. Steinberg, O.M. Auslaender, A. Yacoby, J. Qian, G.A. Fiete, Y. Tserkovnyak, B.I. Halperin, K.W. Baldwin, L.N. Pfeiffer, and K.W. West, *Phys. Rev. B* **73**, 113307 (2006).
- [6] J. Lee, S. Eggert, H. Kim, S.-J. Kahng, H. Shinorara, Y. Kuk, *Phys. Rev. Lett.* **93**, 166403 (2004).
- [7] L.C. Venema, J.W.G. Wildöer, J.W. Janssen, S.J. Tans, H.L.J.T. Tuinstra, L.P. Kouwenhoven, and C. Dekker, *Science* **283**, 52 (1999).
- [8] S.G. Lemay, J.W. Janssen, M. van den Hout, M. Mooij, M.J. Bronikowski, P.A. Willis, R.E. Smalley, L.P. Kouwenhoven, C. Dekker, *Nature* **412**, 617 (2001).
- [9] S. Eggert and I. Affleck, *Phys. Rev. B* **46**, 10866 (1992); *Phys. Rev. Lett.* **75**, 934 (1995).
- [10] M. Fabrizio and A.O. Gogolin, *Phys. Rev. B* **51**, 17827 (1995).
- [11] S. Eggert, H. Johannesson, and A. Mattsson, *Phys. Rev. Lett.* **76**, 1505 (1996).
- [12] A.E. Mattsson, S. Eggert, and H. Johannesson, *Phys. Rev. B* **56**, 15615 (1997).
- [13] V. Meden, W. Metzner, U. Schollwöck, O. Schneider, T. Stauber, and K. Schönhammer, *Eur. Phys. B* **16**, 631 (2000).
- [14] S. Eggert, *Phys. Rev. Lett.* **84**, 4413 (2000)
- [15] P. Kakashvili, H. Johannesson, and S. Eggert, *Phys. Rev. B* **74**, 085114 (2006).
- [16] F. Anfuso and S. Eggert, *Phys. Rev. B* **68**, 241301(R) (2003)
- [17] H. Benthien, F. Gebhard, and E. Jeckelmann, *Phys. Rev. Lett.* **92**, 256401 (2004).
- [18] S.R. White, *Phys. Rev. Lett.* **69**, 2863 (1992); *Phys. Rev. B* **48**, 10345 (1993).
- [19] For a review see S. Eggert, *Theoretical Survey of One Dimensional Wire Systems*, edited by Y. Kuk, et al. (Sowha Publishing, Seoul, 2007), p. 13; arXiv:0708.0003.
- [20] K. Schönhammer and V. Meden, *Phys. Rev. B* **47**, 16205 (1993).
- [21] G.L.G. Sleijpen and H.A. van der Vorst, *SIAM J. Matrix Anal. Appl.* **17**, 401 (1996); J.J. Dorando, J. Hachmann, and G.K.L. Chan, *J. Chem. Phys.* **127**, 084109 (2007).
- [22] I. Schneider and S. Eggert, unpublished.